Schweizerische Eidgenossenschaft
Confédération suisse
Confederazione Svizzera
Confederaziun svizra

Department of the Environment, Transport, Energy and Communication DETEC

Swiss Federal Office of Energy SFOE
Energy Research

Final report

Conception novatrice du rotor d'un nouveau système éolien aéroporté

Innovative rotor design of a new airborne wind power system

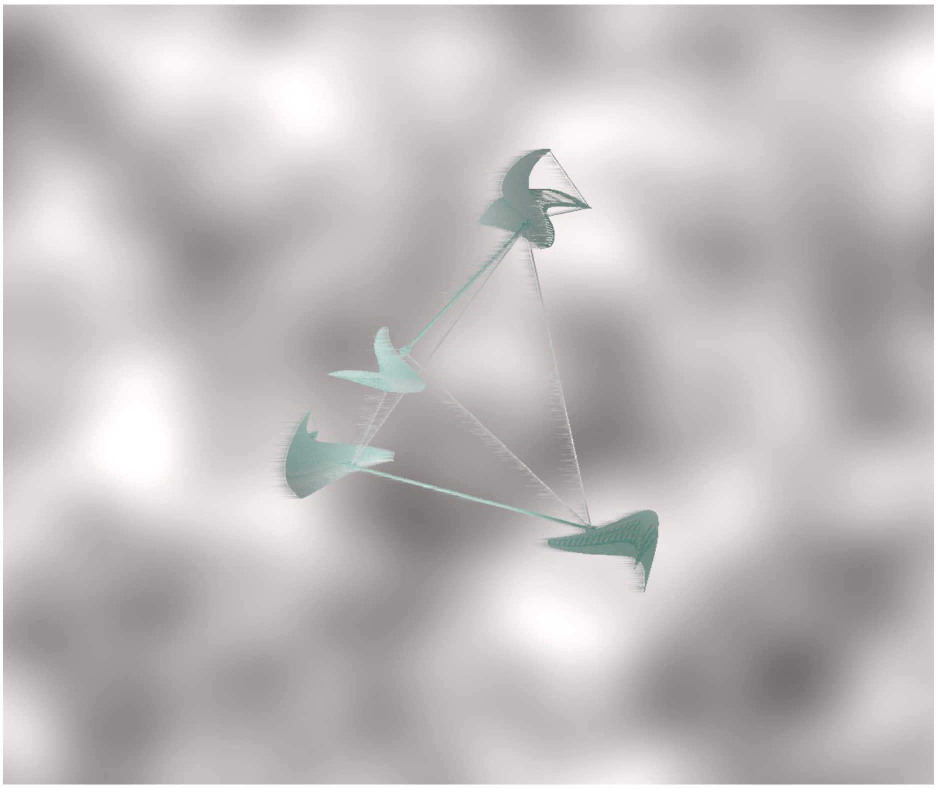

Representation of "Wing-Kite" semi-flexible blades operation in two stages of vertical Zarawind rotor.
The blades are passively deployed as kite in downwind motion and then folded as wing in upwind motion.

Date: 04.05.2020
Town: Bern

Publisher:
Swiss Federal Office of Energy SFOE
Wind Energy Research Programme
CH-3003 Bern
www.bfe.admin.ch

Agent:
ZHAW, Zurich University of Applied Sciences
School of Engineering
Technikumstrasse 9, CH-8400, Winterthur
www.zhaw.ch

Zarawind
Wildbachstrasse 20, CH-8400, Winterthur
www.zarawind.com

Author:
Y. Safa, ZHAW, safa@zhaw.ch

SFOE head of domain: L. Perret, lionel.perret@planair.ch

SFOE programme manager: K. Maus, katja.maus@bfe.admin.ch

SFOE contract number: SI/501823

Swiss Federal Office of Energy SFOE
Mühlestrasse 4, CH-3063 Ittigen; postal address: CH-3003 Bern
Phone +41 58 462 56 11 · Fax +41 58 463 25 00 · contact@bfe.admin.ch · www.bfe.admin.ch

Contents

List of abbreviations

AWE	Airborne Wind Energy
LTA	Lighter-Than-Air
VAWT	Vertical axis wind turbine

Resumé

À plusieurs centaines de mètres d'altitude dans le ciel, les courants de vent sont plus forts et beaucoup plus réguliers que ceux qui sont proches du niveau du sol. Pour récolter la forte énergie du vent à cette altitude, un aérostat à gaz flottant est utilisé pour soulever un générateur électrique. Désigné par "éolienne plus légère que l'air", le système flotte dans le ciel et envoie l'électricité à la terre via un câble de connexion. Un nouveau concept d'éolien aéroporté est ainsi introduit par Zarawind, une spin-off de la ZHAW, l'université des sciences appliquées de Zürich, basée à Winterthur. L'efficacité de ce concept vient du fait qu'il maintient le système aéroporté en position stationnaire à haute altitude en assurant une récolte efficace de la forte énergie éolienne. En raison de son applicabilité presque partout dans de vastes zones économiques de vents forts à hautes altitudes, une potentielle exploitation de cette technologie est prévue comme_une source d'énergie écologique, rentable et mise à échelle dans des zones hors réseau d'électricité. Dans ce projet de recherche, une caractérisation aérodynamique d'un concept de pale de rotor novatrice est introduite. Les influences de la géométrie sont étudiées et les propriétés des matériaux sont analysées en vue de développer la performance et la durabilité d'une éolienne aéroportée plus légère que l'air. Les tâches de la recherche combinent des simulations numériques, des tests de matériaux, des constructions de modèles, des expériences en soufflerie et des travaux de conception-analyse d'ingénierie. Les résultats obtenus devraient faciliter l'évaluation de l'efficacité du système et d'élaborer une ligne directrice pour une implantation d'un nouveau prototype.

Summary

At several hundred meters above ground level, wind currents are stronger and much more consistent than those close to the ground. To harvest strong wind power at that elevation, a buoyant gas aerostat is used to lift up an electrical generator. Denoted by "Lighter-Than-Air (LTA) wind power turbine", the system hovers in the sky and sends electricity through a cable-tether connection to the earth. A new LTA wind turbine concept is introduced by Zarawind, Winterthur-based spin-off ZHAW Zürich University of Applied Sciences. The efficiency of this concept comes from the fact that it maintains the airborne system stationary operating at high altitude with an efficient harvesting of the strong wind power. Among many others, this technology is advantageous due to the applicable deployment of the efficient buoyant airborne system in the wide economic areas of the high-altitude strong-winds. This promotes potential exploitation of this technology as an eco-friendly, cost-effective and scalable power source in off-grid zones. In this research project, we characterize the aerodynamics of an innovative blade concept for LTA wind power turbine, we study the influences of the geometry on the performance of the new wind power rotor, we analyze the durability of rotor's materials. The research tasks combine numerical simulations, material tests, model constructions, wind tunnel experiments, and engineering design-analysis works. Obtained results should facilitate evaluation the system efficiency and developing a guideline design of a new prototype.

1. Introduction

Classical wind power systems are not always an applicable energy solution in regions where winds are not sufficiently strong at the altitude of classical windmills. On the other hand, at several hundred meters above ground level, winds are stronger and much more consistent. To harvest such a strong wind power, Zarawind presents a new concept of a wind power rotor-generator system carried by an aerostat to send electricity through a tether-cable connection to the ground. The efficiency of this concept comes from the facts: first, the system can be maintained at high altitudes independently from wind conditions, second, it ensures a continuous and economic harvesting of the wind power at high performance coefficient. This is based on an innovative vertical counter-rotating rotor the first implemented using flexible blade which operates with passive folding and deployment promoting the aerodynamic performance.
Moreover, the rotor produces an upward-thrust force Fig. 1, this force counters the tether curvature effects in strong winds. Those innovative benefits are satisfied in the designed system at reduced payload installation costs. Indeed, the omni-directional vertical rotor is built-up through a tensional-integrity (tensegrity) concept. This ensures a reliable toque transmission through rotor stages at reduced-mass components that are bending and shear free. As such, the rotor can maintain a high power performance at controlled payload of the buoyant system.
In the real conditions of wind flow, buoyant aerostat, rotor, and tether cable are exposed to aerodynamic drag forces. This denotes an inevitable inclination of the vertical tethered rotor. Competitive effects between tether-traction, tether-cable load, and aerostat forces govern the curved-shape of the tether Fig. 1. Indeed the tether angle exhibits variation from the aerostat confluence point level to the ground mooring (attachment) point. Investigation of different aerostat models, stated that tether angle could range from zero in "no-wind", until 45 degrees in strong winds (30 Km/h) depending on aerostat models.
However, uncontrolled tether-inclination (or curvature) could affect the rotor performance when the airborne tethered system is blowing down to lower-wind-speed altitudes. We recall that advantageous feature of the technology relies on system positioning at high-altitude strong wind capacity. To ensure a stationary positioning of the aerostat at higher altitudes, one can suggest to over-design the buoyant volume, this increases however, the installation costs of the system.

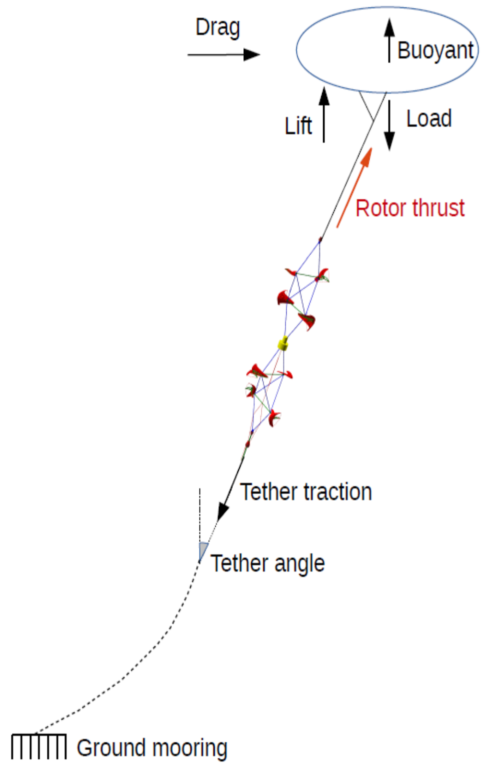

Figure 1: forces' equilibrium of Zarawind system hovering at high-altitudes. Upward rotor-produced thrust counters tether-curvature and helps against system blowing-down in stronger winds.

1.1. Innovative solution

Step-forward is achieved by Zarawind LTA wind power turbine through the introduction of "wing-kite blade" concept. Specifically, the rotor can generate enhanced power from both drag-driven and lift-driven rotation. Moreover, the wind power rotor is not a zero-lift component in the airborne system. In contrast, the rotor produces an upward thrust force Fig.1. When winds speed-up, this force counters a substantial part of the drag increases effects. This contributes to a stationary positioning of the floating system at high-altitude with controlled investment in aerostat volume design.
To provide such a service, the rotor is designed like a bionic-inspired concept where blades mimic the birds interaction with winds. The novel "wing-kite blade" operates as follows: in downwind motion, blade is passively

deployed to take a kite configuration producing both drag forces (driving rotation) and lift forces. The flexible blade is passively folded in upwind motion to take wing configuration producing lift forces driving rotation and elevation. The mechanism of new rotor with “Wing-Kite Blade” concept is explained through two operational stages:

- ***Starting stage with flapping mode:*** during this stage, aerostat starts blowing-up strongly at low altitudes in a moderate wind speed medium. The tether angle is limited and the rotor is quasi-vertical or slightly inclined and operating at low TSR (Tip Speed Ratio). This facilitates blade alternation between kite configuration in downwind-motion and wing configuration in upwind-motion Fig. 2 (a). During this stage, the rotor is mostly kite-drag-driven and partially wing-lift-driven operating.

- **Fast-rotation stage with soaring mode:** at higher altitudes strong winds increase the tether-angle value due to drag effects. Hence the rotor gets more inclined and operating at higher TSR. With such a fast-rotation at strong inclination, the blade preserves passively the wing configuration in both downwind and upwind motion Fig. 2 (b). During this stage the rotor is mostly lift-driven operating.

In both aforementioned modes (flapping and soaring) upward rotor thrust and power are generated. It is worth to note that one of the interesting features of this mechanism is that vertical rotor is self-starting. Such a self-starting capability is ensured passively during the starting stage, it is produced from the passive deployment of the blade with a kite configuration in downwind motion. Such deployment produces kite-drag forces generating sufficient starting torque without needs to install any on-board active starting devices.

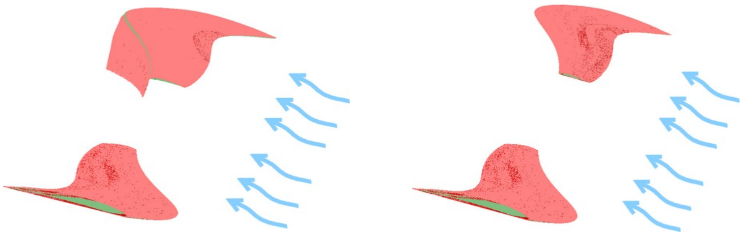

(a) Starting stage: flapping mode (b) Fast-rotation stage: soaring mode

Figure 2: two operational modes of vertical rotor: (a) low altitude flapping mode, (b) high altitude soaring mode

For a successful implementation of the technology, the rotor should insure a threshold aerodynamic performance. Researches and developments are aimed to answer questions on the effect of new blade geometry like: How can blade aerodynamics be affected by rotor inclination in strong winds ?
How can blade change and improve its passive operational modes at high wind speed ? What is the compromise between blade power and payload costs ?

2. Project objectives and accomplishments

In the current stage of innovation-road map, focus is made on characterizing and developing the aerodynamic of new vertical rotor to generate electrical power and aerodynamic lift. This development task is based on numerical simulations, material tests, and wind tunnel experiments. The influences of the geometry on the rotor performance are analyzed in order to optimize the blade design. In this project, obtained results serve to improve the blade design and to develop the functional and the structural integrity of a new prototype model (in ongoing implementation). Accomplished works in the project, make advances in the innovative vision with the airborne wind energy initiative at ZHAW, Zürich University of Applied Sciences. The works belong to three principal tasks accomplished by three teams in the School of Engineering at ZHAW:

- Aerodynamic modeling and numerical simulation at ICP, Institute of Computational Physics
- Wind tunnel tests at ZAV, Center of Aviation
- Material tests and characterization at IMPE, Institute of Material Process and Engineering.

2.1. Preliminary analytical modeling

Before discussing experimental and simulation results, an analytical model of the aerodynamic performance of "Wing-Kite Blade" in the vertical rotor of LTA wind power turbine has been formulated. This model can be informed from measured lift and drag coefficients values of wing and kite. This provides a semi-empirical approach that facilitates highlighting very promising values of rotor power performance, and elevation forces contributed to the system. We consider a kite-shaped blade moving downwind in an inclined rotor Fig. 3. The free-stream, induced and apparent velocities are parameterized with respect to tether angle ξ and flow angle Φ as follows:

$$V=\begin{pmatrix} v \\ 0 \end{pmatrix}, U=u\begin{pmatrix} -\cos(\xi) \\ \sin(\xi) \end{pmatrix}, W=w\begin{pmatrix} \cos(\Phi-\xi) \\ \sin(\Phi-\xi) \end{pmatrix}.$$

At 90º rotor azimuth angle, the total power coefficient of the rotor contributed by both kite downwind Fig. 3 and wing upwind Fig. 4 is obtained as follows:

$$C_p=\lambda\left(1+\lambda^2-2\lambda\cos(\xi)\right)^{1/2}\left(-C_K^l\sin(\xi)-C_K^d(\lambda-\cos(\xi))\right)+\frac{1}{2}\lambda\left(1+\lambda^2+2\lambda\cos(\xi)\right)^{1/2}\left(C_W^l\sin(\xi)-C_W^d(\lambda+\cos(\xi))\right).$$

here $\lambda=u/v$ is the tip speed ratio, C_K^l and C_K^d are the kite lift and drag coefficients.

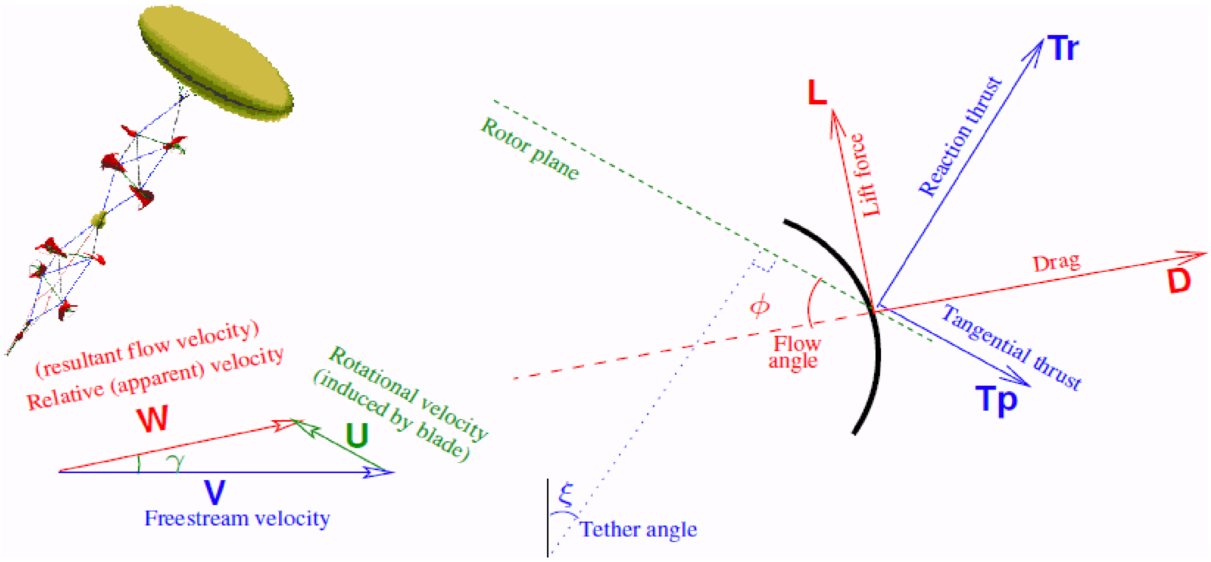

Figure 3: aerodynamic representation of a downwind-moving kite in an inclined tethered-rotor of LTA wind turbine

For C_K^l = 1,33 and C_K^d = 0.8, the power coefficient of the rotor is obtained as function of the tether angle and tip speed ratio as shown in Fig.5 The above preliminary analysis indicates an interesting outcomes with improved lift-drag coefficient of the wing C_W^l = 1,5 and C_W^d = 0.05, the rotor present a higher performance Cp=35 % Fig.5 (right) compared to Fig.5 (left) where the maximum values of Cp=15 % for C_W^l = 1,0 and C_W^d = 0.1. This point out the interesting outcome resulting from the wing aerodynamic performance. Moreover optimal value of tip-speed ratio λ_{opt} > 2/3 for $20<\xi<30$ is predicted by this preliminary analysis at improved wing lift-drag coefficients. This provides option to design a generator with higher RPM at a very lower load. Similar analysis is conducted on the thrust force of the rotor. Considering wind density ρ = 1.2 Kg/m³ and wing swept area A_W = 0.5 m² (half of kite swept area) and wind speed v = 7 m/sec. The total traction thrust of the rotor is shown in Fig. 6. The preliminary analysis states an expectation of aintersting thrust forces per swept area of 4 Kg/m² produced aat higher values of λ_{opt} > 0.5 (high RPM generator) for tether-angle of $20<\xi<30$. Note that such tether-angle interval can be ensured in strong winds using advanced models of tethered-aerostats that can still hovering in the sky at high lift-to-drag ratio.

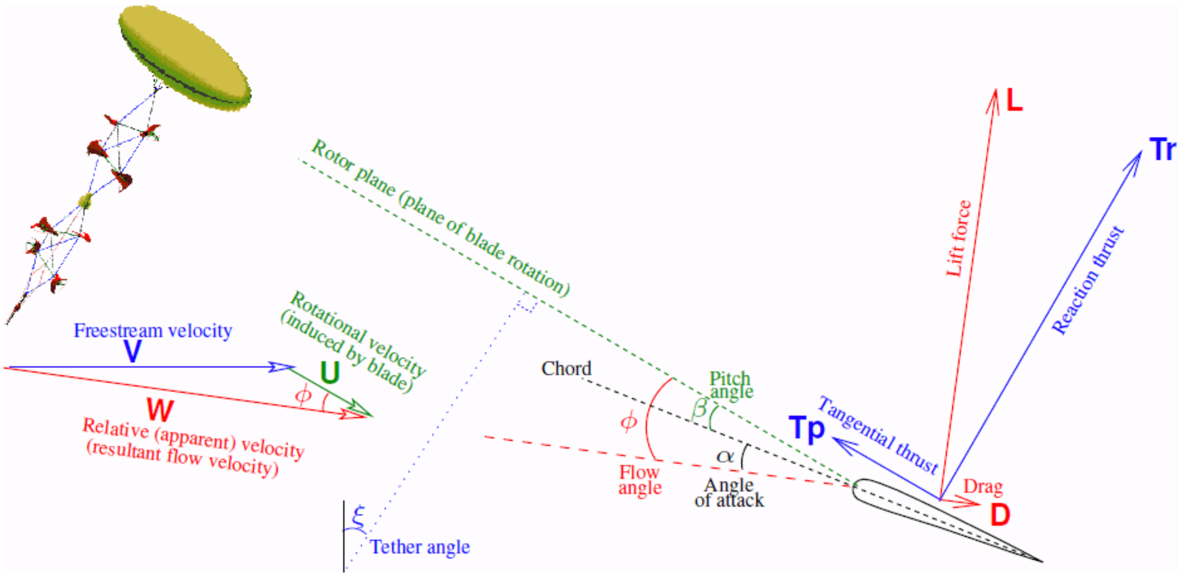

Figure 4: aerodynamic representation of an upwind-moving wing in an inclined tethered-rotor of LTA wind turbine

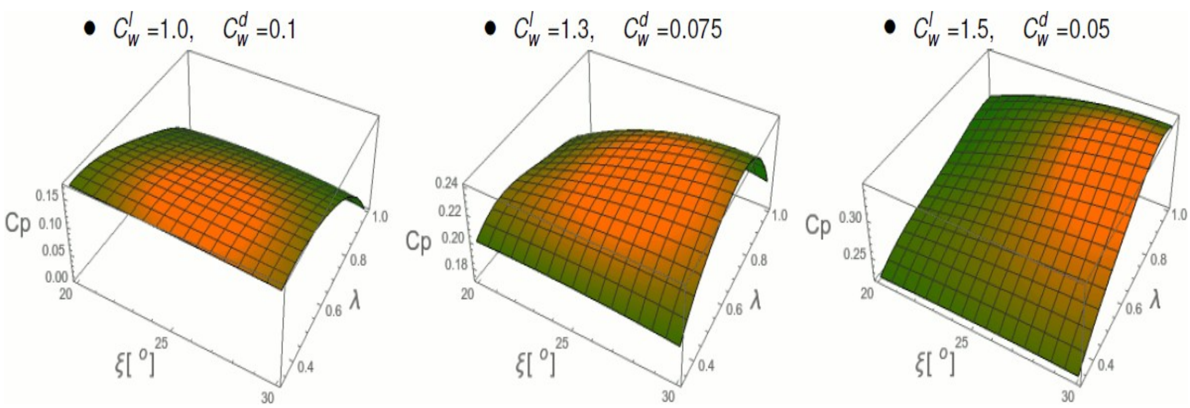

Figure 5: Performance coefficient of the rotor(Mathematica drawing). Highlighted zones correspond to Angle Of Attack (AOA) ranges below stall attributed to different assumed values wing lift-drag coefficients.

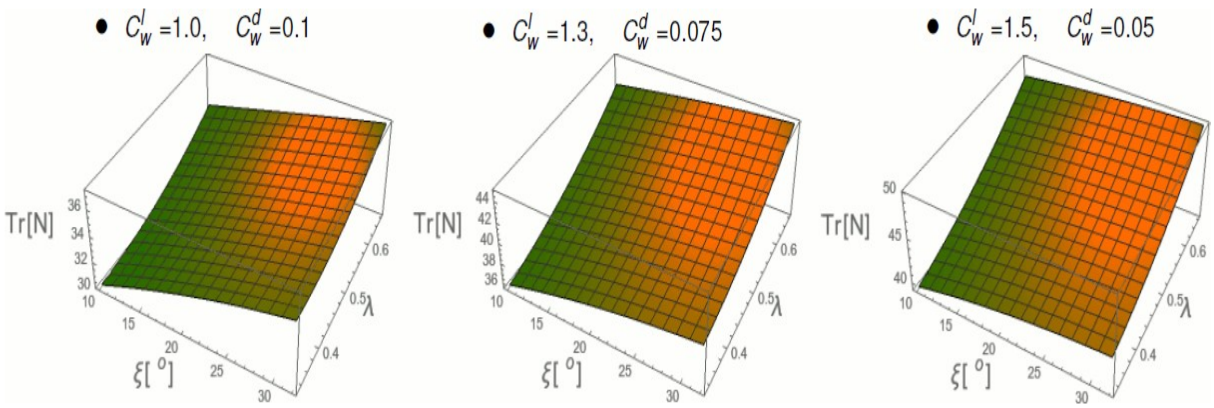

Figure 6: Total traction force (lifting capability) of the rotor for different values of wing lift-drag coefficients. Highlighted zones correspond to high Angle Of Attack ranges below stall attributed to assumed lift-drag coefficients.

2.1. Computational modeling

Studying the new rotor system in term of functional integrity and structural integrity is extremely costing when it is done through extended series of experiments. Hence numerical simulations play a fruitful role in the project to analyze the new rotor in term of power performance and mechanical robustness.

Advanced computational models are set up at ICP Institute of Computational Physics at ZHAW. OpenFoam model is used for the aerodynamic characterization of the rotor. The model treats the cases of internal and external flow around the blade at a Reynolds number Re=10^5. The simulation method provides prediction of pressure and velocity distributions and serves for a reliable estimation of wind loading forces. The applied OpenFoam routine of stead flow (simpleFoam) is an incompressible flow model, it solves for pressure normalized by the density hence $(kg/(m.s^2))/(kg/m^2)=m^2/s^2$. Simulation results on pressure fields in both wing and kite shape are showing suction and compressive pressure contributions to generate wing lift Fig.7 and kite drag and lift Fig.9. The velocity field around the wing, kite and rotor are visualized in Fig. 8, 9 and 10. The traces of pressure field on the rotor surface are shown in Fig. 11.

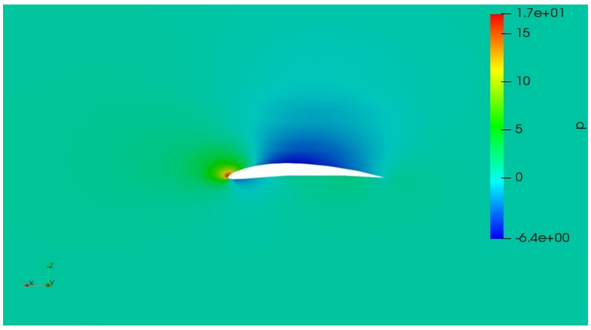

Figure 7: Pressure normalized (m^2/s^2) distribution around the blade in wing configuration

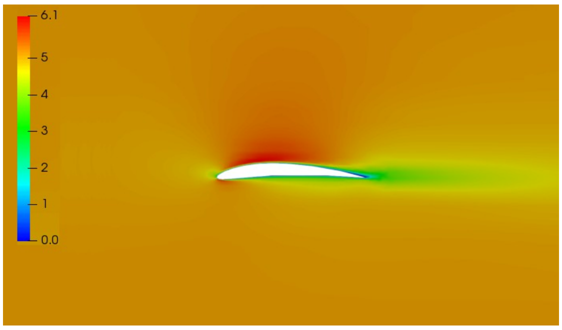

Figure 8: Velocity fields (m/s) distribution around the blade in wing configuration

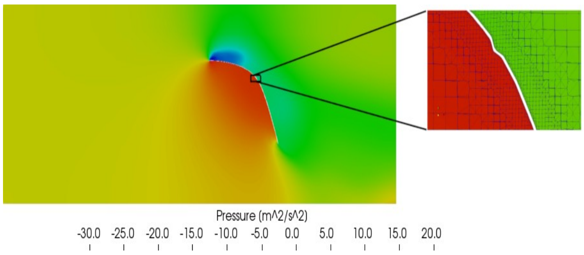

Figure 9: Pressure filed around the blade in kite-configuration exposed to wind flow at 17 degree AOA. Pressure is given in reduced dimension A zoom-in showing local mesh refinement in boundary layer region

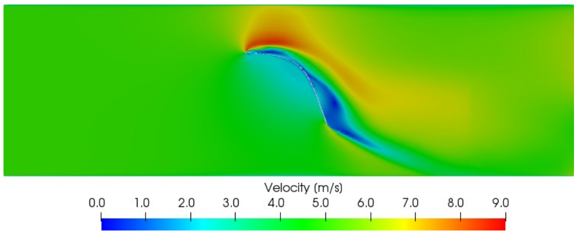

Figure 10: velocity magnitude around the blade in kite-configuration exposed to wind flow at 17 degree AOA.

In aforementioned works, super-computing facilities are used to deal with the large computational size of the treated problems in term of time and memory. For instance the simulation of kite wind tunnel test case was conducted using 1446027 cells, 30 processors, at 39000 steps with clock time: 66000 sec (on cloud). The simulation of the rotor wind tunnel test case was conducted using 3458956 cells, 32 processors, at 20000 steps with clock time: 34000 sec.

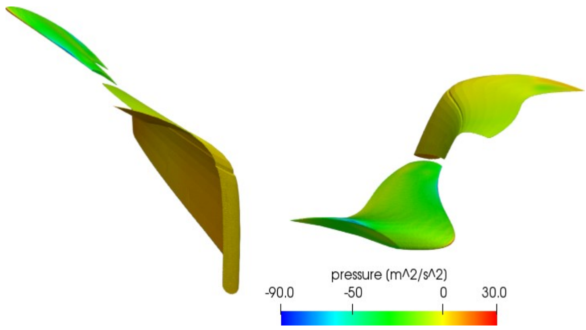

Figure 11: Rotor shown in two azimuths with pressure fields on the surface of the wing and the kite

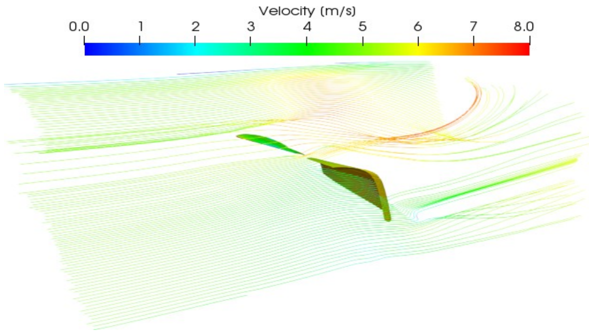

Figure 12: streamlines and velocity of the wind flow through the rotor

The obtained results are validated with respect to experiments. Validation is conducted through comparison of calculated and measured drag and lift coefficients at different angle of attack values Figs. 13, 14.

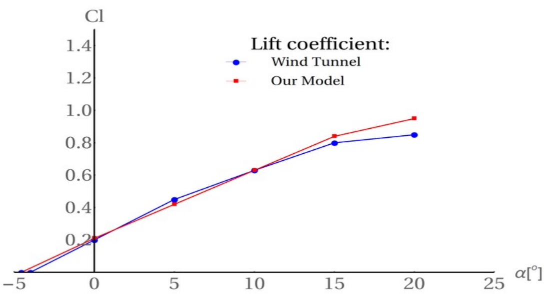

Figure 13: lift coefficient of the wing model for different values of the AOA. Plotted values are obtained from simulations and wind tunnel measurements

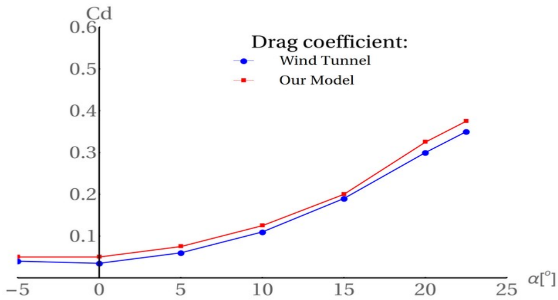

Figure 14: drag coefficient of the wing model for different values of the AOA. Plotted values are obtained simulations and wind tunnel measurements

Model validation allowed us to investigate geometrical parameters affecting lift and drag coefficients of the blade. This is handled through series of tests cases at different of selected airfoil. It is stated that primary model of wing kite blade is suitable to achieve higher performance at increased span-to-chord Aspect Ratio AR Fig.15. As Such observations among others from CFD works provides simulation-based advice on developing blades design for improved aerodynamic performances of the rotor.

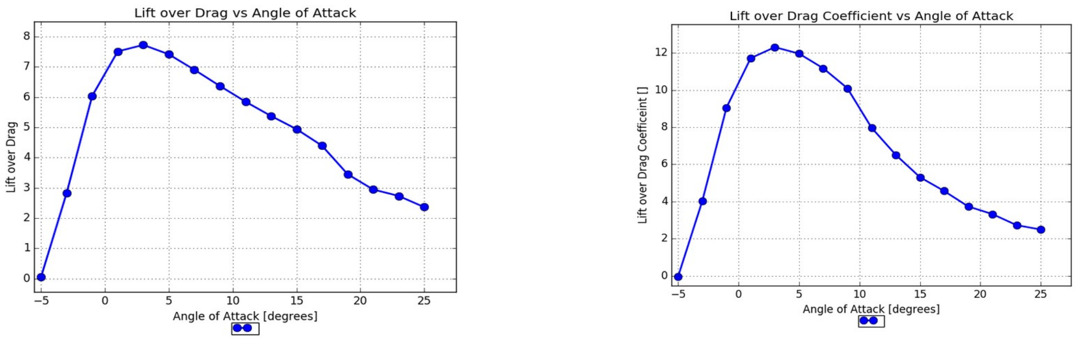

Figure 15: Lift-to-drag values for blade model with span-to-chord Aspect Ratio AR = 3/2 (left) and for AR=9/2 (right)

2.2-Aerodynamic experiments

2.2.1 Single-blade wind tunnel model

A blade model combining both wing and kite functionalities is constructed and then tested in the wind tunnel. The group from ZAV Zentrum für Aviatik at ZHAW are conducting the wind tunnel measurements on this new concept of "wing-kite" blade. The model is tested at different conditions of wind speed (ranging from 6 to 12 m/s) with

varied pitch and Yaw angles. Even-though that tested model represents only the first designed prototype, it is shown that innovative “wing-kite blade” has potential to generates substantial power and contributes furthermore, a considerable elevation (lift) to the airborne system. Obtained results validate the expected values. This gives insight for further developed design to support the realization of the prototype.
Note that by testing two different scales of single-blade model, we have insured further qualitative-estimated control on the blockage effects in the wind tunnel measurements.

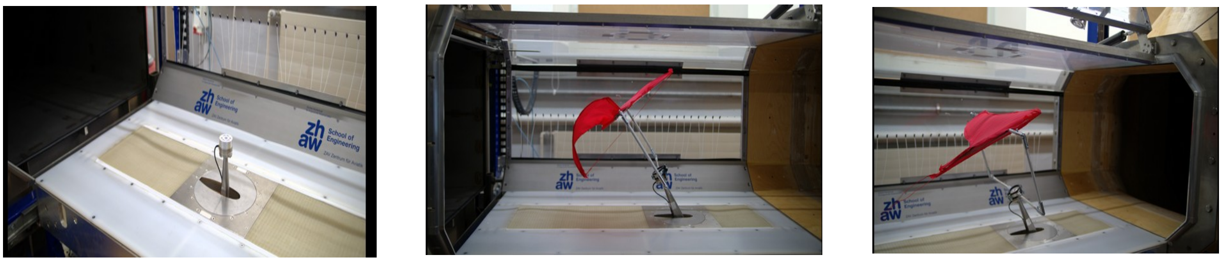

(a) (b) (c)

Figure 16: (a) sensor device mounted for the wind tunnel measurements at Zentrum für Aviatik ZAV, ZHAW, (b) Blade model tested in downwind with kite configuration, (c) Blade model tested in upwind with wing configuration

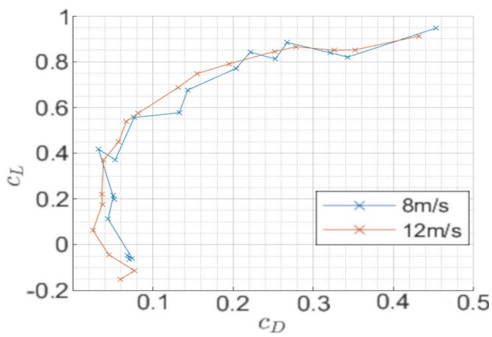

Figure 17: measurements of Lift and drag coefficients for wing configuration at wind speed of 8 and 12 m/sec with different angle of attack.

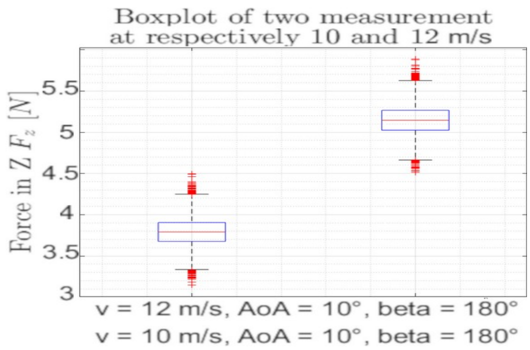

Figure 18: Range of lifting measurements at different AoA, Yaw and wind speed

2.2.2 Static-rotor wind tunnel model

A model of two-arm vertical rotor is set up for testing in the wind tunnel. A static installation of the rotor has been conducted at different azimuth angles and with different wind speed values. In order to examine the effect of the tether inclination in the sky, the rotor is installed with an inclined axis toward downwind. A series of tests at different inclination-angles allowed investigation of torque and lifting at different Angle-Of-Attack AOA. Fig. 18.

2.2.3 Wind tunnel model of dynamic (rotating) rotor

Wind tunnel measurements are being conducted on a rotor rotating at a range of RPM (Rotation Per Minute) and exposed to free stream wind speed values of 8 m/sec. The works are dealing with different set up conditions: installing two and three blade rotor, applying different inclinations of the vertical rotor in down wind to mimic tether angle effects, . The tests are performed using two different models of equipment and measurement devices (torque sensor Datum Electronics, M425 torque transducer, micro motor, speed controller...).

Quasi-static measurements

In the first step, we started measurements at very low rotational speed of the two-blade rotor exposed to free-stream wind speed values of 10 and 12 m/s. The tests were performed on two-blade rotor in the set-up of static model. The results introduced in Fig.19 provide promised lifting capability of rotor.

Fast-rotaion measurements

The tests are performed at higher angular velocity ranging from 10 to 210 RPM with different inclination of two and three-blade model Fig. 20. The results shown in Fig. 21 make clear the advantageous efficiency of three-blade model by presenting double power produced by two-blade model. Note that those measurements were conducted on a starting stage of the rotor operating with flapping (wing-kite) mode. The results shown in Fig. 22 provide some interesting outputs. Indeed at low inclination (8 degrees) the rotor is mostly drag-driven with wing-kite operational mode disposing a very low value of optimal TSR . At strong inclination with 28 degrees the flapping mechanism was not possible. Hence rotor was operating as wing-wing modes disposing higher value of optimal TSR. This explains expectation on rotor mechanism associated with increased wind speed that causes further tether-angle. A transition from flapping stage to lift-driven stage promotes rotor operation at higher TSR. This makes a promising room of developments to benefit from:

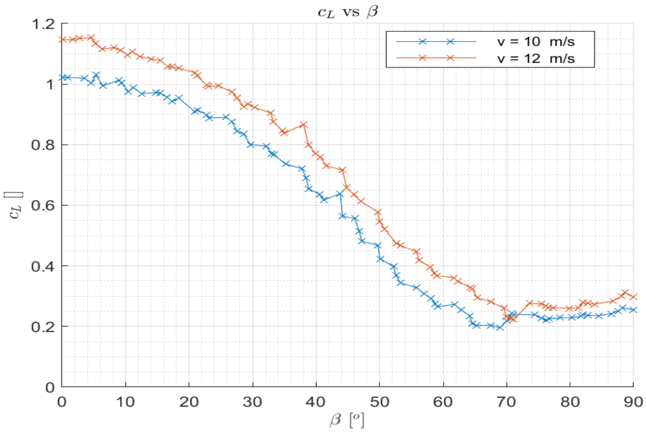

Figure 19: lift coefficient of the rotor for an interval of Yaw angles (0,90 degree). Tested at very low rotational speed.

- Using a reduced mass generator operating at higher RPM at economized buoyant investment.
- Targeting higher power coefficient at higher TSR values of lift-driven mode operation

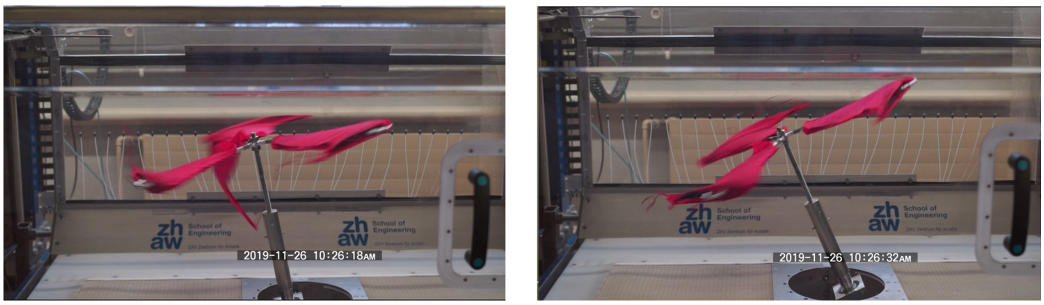

Figure 20: Dynamic (rotating) three-blade rotor in wind tunnel tests. Increased inclination makes transition from flapping mode rotation (left) to soaring mode rotation at the same TSR.

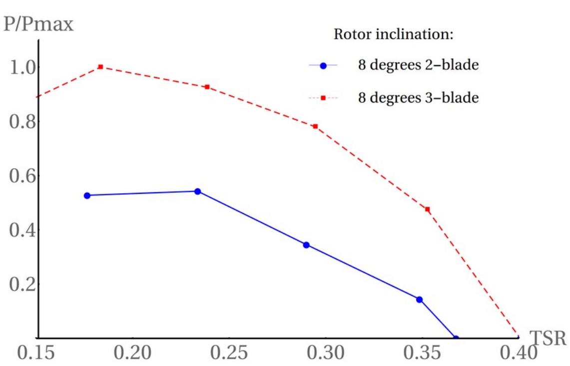

Figure 21: Normalized power for two-blade and three-blade rotor model obtained at same values of Tip-Speed-Ratio TSR. Rotor is operating only with flapping- mode

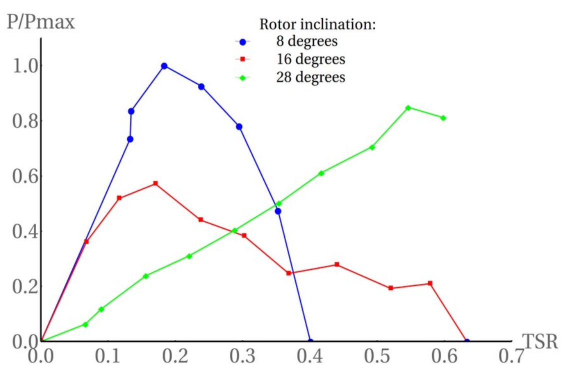

Figure 22: Normalized power for a three-blade rotor model at different installation modes with: inclinations 8 degrees (flapping mode), 16 degrees (flapping stage and then soaring mode) and 28 degrees (soaring mode)

<u>Measurements limitations and purposes</u>

We note that due to small wind tunnel section size, the blade geometry was constrained by a short span. With such conditions we had a-priory expectation of strong lift-induced drag effects. This decreases the aerodynamic efficiency of the wing (see Fig.17) and reduces therefore the magnitude of measured power. However the dynamic tests with such conditions still are meaningful for several purposes like

- Validate the analytical expectations of aerodynamic performance of the rotor.
- Identify threshold values of TSR (Tip Speed Ratio) and rotor inclination (pitch) triggering transition from starting stage (flapping mode) to fast rotational stage (soaring mode) Fig.22.
- Identify optimal values of TSR for starting stage (flapping mode) to rated speed (soaring mode).
- Connclude on the blade geometry developments.

2.2.4 In and out-door trial tests with on-ground installations

For a realistic testing and evaluation of the rotor with “wing-kite blade” mechanism, several in and out-door tests are conducted on the new rotor model. This include tests on model of 16 struts stages to evaluate the torque transmission through tensegrity structure of the rotor. Two scales of vertical rotors were also tested.

The trials were conducted on the ground where blade is deployed to take kite shape in down-wind and then folded-up to take the wing shape in up-wind. This successful operation of wing-kite is realized passively (without external control devices). Obtained results and observations make a strongly fruitful know-how to insure a safe and efficient performance before flying the rotor.

2.3- Material tests and design:

At IMPE Institute of Material Process and Engineering at ZHAW, different materials used for the construction of the rotor are tested. The studied materials includes carbon fibers and fiberglass (used in blade fabrication).

In this report we make focus on the testing results on Dyneema tether materials Fig.23. Note also that Dyneema is light weight strong material used in the tether connection of the flying rotor to the ground.

(a) (b) (c) (d)

Figure 23: Dyneema DSK99 Ultra (a) strands (b) specific weight 3.6 grams/m, 3 mm diameter, tensile strength: 1186 Kg. Ideal for moored aerostat. Testing devices at IMPE ZHAW: Single cantilever bend (c). Film clamp pull (d).

It is important whether the proposed materials can withstand cylic dynamicloading for more than a million times without damage. For this reason, a long-term load tests are performed with the DMA Dynamic Mechanical Analysis. The materials were cyclically loaded with 120 Hz for three hours. We tested at room temperature and at -20 °C to simulate the climatic conditions at high altitudes. In addition, we tested the materials over a wide temperature range in order to set boundary conditions for the operating parameters.

2.3.1 Temperature ramp tests

At temperatures below -50 °C the material becomes brittle. Otherwise, we found no serious changes in the mechanical properties of the material over the measuring range Fig. 24 (a). On the other hand, Dyneema DSK99 Ultra shows a mostly constant stiffness over the entire temperature range Fig.25 (b) . Therefore, it can be used without restriction.

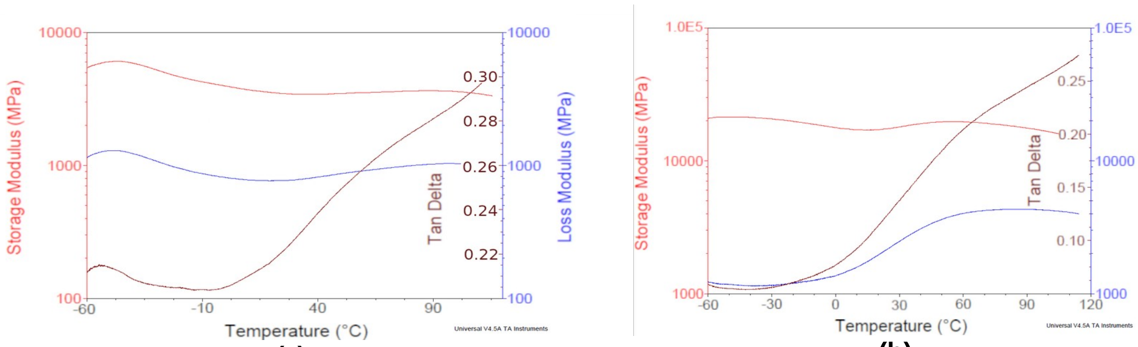

(a) (b)

Figure 24: DMA measurement at IMPE ZHAW, long-term test at -20 °C. Red; storage module. Blue; loss module. Brown; Tan Delta. (a): curves of Dyneema D.PRO DSK78, (b) curves of Dyneema D.PRO DSK99

2.3.2 Long-term test

In this experiment, the samples are cyclically loaded at 120 Hz for 180 minutes (resulting in $1.296*10^6$ operations) Figs. 25 (a, b), 26 (a, b). The test determines whether a decrease in the mechanical properties is apparent. The results provide information whether the materials are able to withstand the permanent cyclic loading. The sample were tempered in the "tempering" area of the measurement. This range does not have a constant temperature and can be ignored.

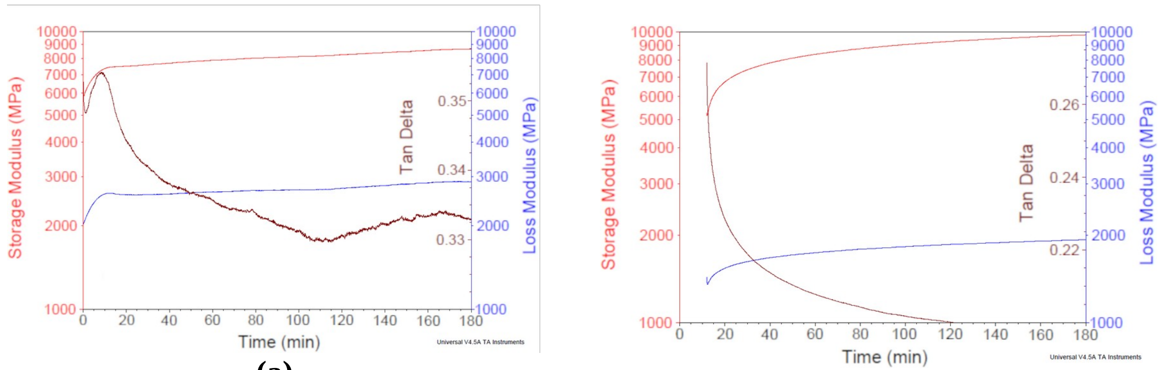

(a) (b)

Figure 25: DMA measurements of Dyneema D.PRO DSK78 long-term test. (a): testing at -20 °C. (b): testing at at 25 °C.

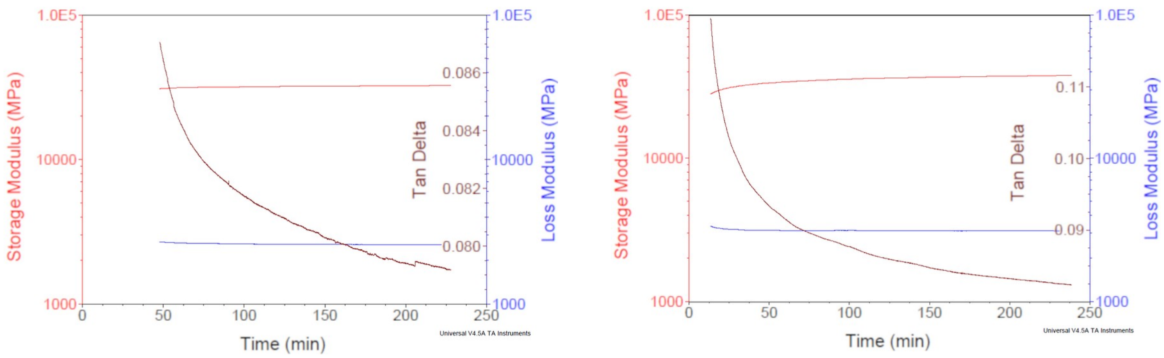

(a) (b)

Figure 26: DMA measurement curve Dyneema D.PRO DSK 99 long-term test.
(a): testing at -20 °C. Red; storage module. Blue; loss module. Brown; TanDelta. (b): testing at at 25 °C.

The sample Dyneema DSK99 Ultra shows a stiffening of the material during the measurement. After almost 1.3 million cycles, no damage to the material was detected.